

Parameter Estimation in Intensity Models for the Maintained Responses of Neurons

Chia-yea Jerry Liu

Charles E. Smith

Abstract: In analyzing the responses of cat auditory brainstem neurons, Johnson et al. (1986, *Hearing Res.* 21: 135-159) developed a point process model to describe the serial dependence between the interspike intervals in the stationary portions of spike-trains. Following his approach, maximum likelihood estimation is examined for one parametric model of the intensity function of the spike-train. The procedures were tested on simulations of the stochastic neural model of Smith & Goldberg (1985, *Biol. Cybernet.* 54:41-51). This model can produce spike-trains that are renewal processes or have a first order dependence. In the renewal case the intensity function is the hazard rate, while the non-renewal case requires a "whitening" procedure via a conditional mean plot analogous to an AR(1) time series model. The concavity of the premedian portion of the hazard rate or "whitened" hazard rate was found to be quite influential both in the specification of the functional form of the intensity and in model verification.

Dept. of Statistics

North Carolina State University

Raleigh, NC 27695

Parameter Estimation in Intensity Models for the Maintained Responses of Neurons

1. Introduction

The phenomenon of spike-trains which are produced by neurons in the nervous system has been extensively studied and reported (see, e.g., Yang and Chen, 1978, and Tuckwell, 1988). It is widely accepted that the temporal pattern of a spike-train, either under external stimuli (*driven*) or not (*spontaneous*), carries important information about both the messages being conveyed through the neuron and the spike generating mechanism of the neuron. The action potentials comprising a spike-train share the same properties of being temporally random, of indistinguishable waveforms, and relatively brief. These properties lead to stochastic point process modeling (Perkel et al., 1967) and statistical analysis of neural spike-trains (Landolt and Correia, 1978).

The main goal of this report is to present an algorithm based on maximum likelihood principles to estimate the parameters contained in the point process model which is used to describe a spike-train. The modeling is through the intensity function of the point process. The proposed algorithm, being conceptually clear as well as easy to interpret, is demonstrated on two simulated spike-train data sets.

The intensity approach to characterize a general point process is sketched out in Section 2. Simulated data sets mimicking auditory-nerve fibers spike-trains are used for computational purposes in this report. They are described in Section 3. Also in Section 3, there is a sequence of data preparation steps to ascertain whether the data satisfies certain requirements of this algorithm before the actual computation is carried out. The algorithm, together with the selected model, is applied to the two artificial spike-trains and the results are summarized in Sections 4 and 5.

2. Intensity Approach

The essence of this approach is to extend the definition of the intensity function of an *inhomogeneous Poisson* process to make it dependent not only on time, but also the history of the process up to that time. In so doing, modeling general point process data, e.g., ones with auto-correlation, becomes more straight-forward. The utility of this approach can also be seen in Yang and Shamma, 1990, where the intensity approach to neural spike-trains was used with simultaneous recordings of multiple neurons to provide estimates of synaptic connectivities.

The counting process of a point process up to time t is denoted by N_t . The corresponding occurrence times are denoted by $\{w_n; n=1,2,\dots,N_t\}$, and the interarrival times by $\{\tau_n; n=1,2,\dots,N_t\}$. The occurrence times and the interarrival times provide exactly the same information about a point process because $\tau_k = w_{k+1} - w_k$, for $k \geq 1$ by definition. For spike-train data, τ_n is also called the n -th interspike interval (ISI), and it is also assumed that $w_0 \equiv 0$.

The intensity function $\lambda(t)$ of an inhomogeneous Poisson process $\{N_t^0; t \geq 0\}$ is defined to satisfy

$$Pr\{N_{t+\delta}^0 - N_t^0 = 1\} = \lambda(t) \cdot \delta + o(\delta),$$

and

$$Pr\{N_{t+\delta}^0 - N_t^0 > 1\} = o(\delta)$$

for some $\delta > 0$. Snyder, 1975, defines a self-exciting point process as one whose intensity function depends on the entire history, denoted by H_t , of the point process up to time t . The intensity function $\lambda(t; H_t)$ now satisfies

$$Pr\{N_{t+\delta} - N_t = 1 | H_t\} = \lambda(t; H_t) \cdot \delta + o(\delta),$$

and

$$Pr\{N_{t+\delta} - N_t > 1 | H_t\} = o(\delta)$$

for some $\delta > 0$ where H_t includes the occurrence times $\{w_n; n=1,2,\dots,N_t\}$ and the number of occurrences N_t of the process up to time t .

Thus defined, the class of *stationary renewal* point processes (see Johnson and Swami, 1983) will have an intensity function of the form

$$\lambda(t; H_t) = f(t - w_{N_t}),$$

where w_{N_t} denotes the last occurrence time of the process up to time t .

We adopt the approach of Johnson and Swami, 1983, to model a stationary renewal point process by decomposing its intensity function into a product of two parts: *signal* and *recovery*. The intensity function of a stationary renewal point process now has the form

$$\lambda(t; H_t) = \begin{cases} \lambda_0 \cdot r(t - w_{N_t}), & \text{if } t - w_{N_t} \geq 0 \\ 0 & , \text{ otherwise} \end{cases}$$

where λ_0 is the constant signal rate and $r(\cdot)$ is the recovery function characterizing the *relative refractory* behavior of the spike-train. Notationally, the intensity function will be simplified to be

$$\lambda(t; H_t) = \lambda_0 \cdot r(t - w_{N_t}).$$

The *absolute refractory period*, or the *dead-time*, is considered fixed in this report. It behaves as a parameter t_d in the intensity function, i.e.,

$$\lambda(t; H_t) = \lambda_0 \cdot r(t - w_{N_t} - t_d).$$

For model selection, in renewal case, the hazard function of the interspike intervals is identical to the intensity function (Snyder, 1975). Therefore the empirical hazard rate plot should give clues as to what the underlying intensity model would be, provided that the spike-train is renewal. This diagnostic step is not always useful because the standard errors for the hazard rate increases as time increases. It is not easy to provide a meaningful fit to the empirical hazard rate when data size is not large enough.

The likelihood function of a spike-train with history H_t and an intensity function $\lambda(t; H_t)$ is

$$L(\theta; H_t) = \exp\left\{-\int_0^t \lambda(s; H_s) ds + \int_0^t \log\{\lambda(s; H_s)\} dN_s\right\}$$

where θ denotes the parameters contained in $\lambda(t; H_t)$ (see Snyder, 1975). The upper limits of the integrals are usually replaced by w_n since no information is available beyond the last occurrence time.

3. Data Preparation Steps

Since only stationary point processes are considered in this report, certain requirements must be met before the maximum likelihood computation can be carried out for the data. If auto-correlation are present, serial dependence is removed by a "whitening" procedure to produce a stationary renewal process. Maximum likelihood estimation is then carried out on this underlying process. Model validation via simulating with estimated parameters and reversing the whitening if necessary follows parameter estimation. The procedures are put together as a flow-chart in Fig. 1. The steps are briefly described as follows:

Step 1. Check stationarity. The Wald-Wolfowitz runs test is used as suggested in Correia and Landolt, 1977. Stop the procedure if the spike-train is not stationary since only stationary point processes are considered. Examples of stationary point processes are spontaneous spike-trains and maintained responses of auditory-nerve fibers (see Kiang et al., 1965).

Step 2. Check independence among ISI's. The correlogram is a useful tool for this purpose. The conditional mean plot is also helpful. If the spike-train shows evidence of auto-correlation, move to *Step 2A*.

Step 2A. Use the conditional interval histograms to determine the type of dependence in the ISI's. When the difference in the conditional interval histograms can be explained solely by the magnitudes of the conditioning intervals, i.e., the difference is no more than a shift in the horizontal axis, a "whitening" procedure somewhat analogous to an AR(1) time series model is used and the transformed ("whitened") spike-train is sent back to *Step 1* again. Details are illustrated in Section 5.

Step 3. Test for the renewal property of the spike-train. The periodogram test (see Cox and Lewis, 1966), or the Bartlett's Kolmogorov-Smirnov test (see Fuller, 1976), is employed together with the conditional interval histograms (see Section 5). One possible way for an independent point process to be non-renewal is that it is a *semi-alternating renewal (SAR)* point process (see Kwaadsteniet, 1982).

Step 4. Select an intensity function and carry out maximum likelihood estimation.

Step 5. Use the estimates of the parameters to simulate data to be compared with the original one. For the non-renewal case, generate a renewal data using the parameter estimates, and then reverse the whitening procedure. Finally compare this resultant spike-train with the original one.

The data sets NERVE1 and NERVE2 are generated using the afterhyperpolarization model of Smith and Goldberg, 1985. Each of them contains 2000 interspike intervals. The Wald-Wolfowitz runs test statistics for them are .0323 and 0.7641, respectively. That is, they are both stationary since the test statistics should be asymptotically normally distributed with mean 0 and variance 1 under the null hypothesis.

The correlogram of NERVE1 as shown in Fig. 2.1.(a) exhibits no strong evidence of auto-correlation of any order. The conditional mean plot in Fig. 2.1.(b) says the same thing. The test statistic of NERVE1 for the periodogram test is 0.0174, implying that NERVE1 is renewal. The conditional interval histograms of NERVE1, as shown in Fig. 3(a), further support its renewal property since there is no significant difference among the histograms. It then can be treated as a stationary renewal process.

The correlogram and the conditional mean plot of NERVE2 (Figs. 2.2.(a) and (b)) support the existence of a negative first order auto-correlation. We then moved to *Step 2A* for the "whitening" procedure. The periodogram test, although unnecessary at this point, is performed on NERVE2 to confirm that the renewal hypothesis is rejected at 0.01 level as expected.

4. The Renewal Case—NERVE1

The selected intensity function is

$$\lambda(t; H_t, \lambda_0, \beta, \alpha) = \lambda_0 \cdot [1 - \exp\{-\left(\frac{t - t_d - w N_t}{\beta}\right)^\alpha\}].$$

It is seen that the model contains a constant signal rate λ_0 , a recovery shape constant α , a recovery time constant β , and the recovery function $r(\cdot)$ exponentially approaches 1. The likelihood equations and the maximum log-likelihoods (m.l.l.) of this model are derived without the dead-time t_d and listed in the Appendix.

Because of the special nature of fixed dead-time parameter in the model, it is possible to consider first the model without the dead-time, and then examine the effect of the dead-time. The model is fitted to data sets NERVE1(j) = { $\tau_n - t_d(j)$; $n=1,2,\dots,2000$ } where { τ_n ; $n=1,2,\dots,2000$ } is the original data set and $t_d(j)$ denotes a value selected for the dead-time within the range

$$D = \{(0, \min \tau_n)\}.$$

Then estimates of other parameters can be evaluated for each dead-time t_d , and the corresponding likelihood evaluated. The maximum likelihood estimates of the parameters, including the dead-time, can be calculated through maximizing the likelihoods with respect to the dead-time. That is, the intensity function $\lambda(t; H_t)$ and the corresponding likelihood function $L(\lambda_0, \alpha, \beta, H_t)$ as defined in Section 2 become indexed by t_d . Then the maximum likelihood estimates $\hat{\lambda}_0$, $\hat{\alpha}$, $\hat{\beta}$, and \hat{t}_d are values such that

$$\max_{t_d \in D} \{ \max_{\theta} L_{t_d}(\theta, H_t) \}$$

is achieved.

For a fixed dead-time value, the first likelihood equation, $\hat{\lambda}_0 = \hat{\lambda}_0(\hat{\alpha}, \hat{\beta})$, defines a smooth surface in the space spanned by $\hat{\lambda}_0$, $\hat{\alpha}$, and $\hat{\beta}$, and hence a surface in the parameter space. It is difficult to illustrate this surface in the parameter space spanned by λ_0 , α , β , and t_d . The numbers listed in Table I should help to visualize how the log-likelihood function varies as each of the parameters changes. The maximum likelihood estimates are $\hat{\lambda}_0=0.1996$, $\hat{\alpha}=2.50$, $\hat{\beta}=7.0$, and $\hat{t}_d=1.87$.

The spike-train simulated using the maximum likelihood estimates is compared with NERVE1. The main evidence validating the model is the Kolmogorov-Smirnov two sample test

result. The test statistic is 1.1068, and the p -value is 0.1641. This test is meaningful here since the spike-train is renewal. The estimated intensity function is plotted over the empirical hazard rate (Fig. 6) to illustrate the degree of fit. The univariate statistics of the two spike-trains show that the skewness of NERVE1 is much greater than that of the one simulated.

5. The Non-renewal Case—NERVE2

When auto-correlation is detected in spike-train data, one would like to determine the order and structure of the correlation. One method, as suggested by Johnson et al., 1986, that is helpful is to plot the *conditional interval histograms* of the spike-train. Conditional interval histograms are plotted as follows: group the pairs of interspike intervals (τ_{k-i}, τ_k) according to the magnitude of the conditioning interval, i.e., the first one in each pair, then plot the histogram of the latter one for each group. The integer i denotes the order of the conditioning, with 1 being the one most frequently used. If the spike-train is renewal, then the conditional interval histograms will be identical. In the non-renewal case, the conditional interval histograms can differ in a number of ways.

There is a special class of spike-trains that produce conditional interval histograms differing only in the location but *not* in shape (see Johnson et al., 1986). It is expected that once the shifting effect contributed by τ_{k-i} is removed from the conditioned intervals τ_k , then the resultant new spike-train will be free of the type of dependence that used to exist between τ_{k-i} and τ_k . This is what exactly a whitening procedure does and creates a whitened spike-train $\{\tau'_n; n \geq 1\}$ that is renewal. One way to determine the effect of the conditioning interval is by computing the conditional expectation of the k -th interspike interval given the $(k-i)$ -th interspike interval. That is,

$$E[|\tau_k| \tau_{k-i}] = C \cdot g(\tau_{k-i})$$

where C is a positive constant. The resultant (whitened) spike-train $\{\tau'_n; n \geq 1\}$ is defined to be

$$\{h[\tau_n - g(\tau_{n-i})]; n \geq 1\},$$

for some function $h(\cdot)$. This implies that the conditional mean plot in *Step 2*, or some plots equivalent to it, can be used to find the function $g(\cdot)$ within a certain range. If $g(\tau_{n-i})$ is nonconstant for some $i > 1$, i.e., higher than first order dependence, then these expectations should be redone simultaneous conditioning on the i previous intervals. This produces a multivariate form for $g(\cdot)$ and hence requires larger data sets. For our example, only first order dependence was indicated.

The correlogram of NERVE2 in Fig. 2.2.(a) shows that first order correlation is the only significant one and the conditional mean plot in Fig. 2.2.(b) shows a nearly linear pattern. The conditional interval histograms in Fig. 4(a) show that nothing more than a shift is observed among the histograms. That is, the above whitening procedure seems appropriate here. In determining the

functional form $g(\cdot)$ mentioned above, for reasons to be discussed in Section 6, a simple linear function in τ_{k-1} is not considered despite that the conditional mean plot is almost perfectly linear over a certain range. Instead, the corresponding conditional mean plot for the pairs $(\tau_{k-1}, \log \tau_k)$ is used and shown in Fig. 5. The ordinary linear regression gave a slope estimate of -0.043. That is

$$E[\log(ISI_n) | \tau_{n-1}] = -0.043 \cdot \tau_{n-1} + C.$$

So the whitened spike-train is defined as

$$\{\tau_n \cdot \exp(0.043 \cdot \tau_{n-1}); n \geq 1\}.$$

The Wald-Wolfowitz runs test gives 1.1568 which is insignificant. The correlogram (Fig. 2.3.(a)), conditional mean plot (Fig. 2.3.(b)), and the conditional interval histograms (Fig. 4(b)) of the whitened NERVE2 all support that the whitening is working. The periodogram test statistics of 0.0275 assures that it is renewal. The whitened spike-train NERVE2 is now ready for maximum likelihood estimation.

The model used here for the whitened NERVE2 is the same as in Section 4. The computed estimates are: $\hat{t}_d=0.5$, $\hat{\alpha}=4.0$, $\hat{\beta}=5.5$, $\hat{\lambda}_0=1.3646$. The behavior of the likelihood surface is summarized in Table II. The spike-train reproduced using this set of parameter estimates and the whitening procedure gives a correlogram (Fig. 2(a)), conditional mean plot (Fig. 2(b), and conditional interval histograms (Fig. 4(c)) that are very similar to those of the original NERVE2.

As for the verification of the identity of two non-renewal spike-trains, there is not a generally established criterion. One possible way to do it is to combine the results of the comparisons between the two sets of conditional interval histograms and the significant correlation coefficients of the two target spike-trains. Since the non-renewal spike-train, NERVE2, was assumed to have a fairly simple correlation structure, the criteria emphasize only on the first order correlation rather than from a general joint distribution point of view (c.f. Cox and Isham, 1980).

6. Discussion

In the last section, despite the obvious linear relationship between τ_n and τ_{n+1} , the function

$$E[\log \tau_{n+1} / \tau_n] = b \cdot \tau_n + C$$

was used for whitening NERVE2 instead of a simple linear regression of τ_{n+1} on τ_n . The reason for this choice is because an exact AR(1) analog whitening procedure is not reversible. That is, if the linear regression model

$$E[\tau_{n+1} / \tau_n] = b \cdot \tau_n + C$$

was used, then the whitened spike-train would be

$$\tau'_n = \tau_n - b \cdot \tau_{n-1}.$$

The whitening will not create any problem if b is negative, i.e. τ'_n will be positive. A negative first order correlation coefficient is often observed in spontaneous spike-trains.

The difficulty occurs when we want to simulate the original spike-train by using estimates of the regression parameters and reversing the whitening procedure, i.e., taking

$$\tau_n = \tau'_n + b \cdot \tau_{n-1}.$$

This equation does not guarantee that τ_n is a positive random variable since b is negative. One way to try to circumvent this difficulty was outlined in Section 5.

When a point process is renewal, its intensity function is identical to its hazard function (see Snyder, 1975), thus the shape of the hazard rate of a spike-train has a major impact on the selection of the intensity model in the algorithm proposed in this report. As stated in Section 4, the constants governing the shape of the hypothesized intensity function need to be estimated. From the hazard rate plot, we can determine possible ranges for the constants and then proceed with a grid-search procedure.

Appendix: Derivation of Likelihood Equations

Without loss of generality, the dead-time t_d will be dropped from the intensity function for this derivation.

$$\lambda(t; H_t) = \lambda_0 \cdot (1 - \exp\{-[(t - w_{N_t})/\beta]^\alpha\}),$$

$$\begin{aligned} \log L(\lambda_0, \alpha, \beta | H_t) &= -\sum_{i=1}^n \int_0^{\tau_i} \lambda_0 \cdot (1 - \exp(-[t/\beta]^\alpha)) dt + \sum_{i=1}^n \log\{\lambda_0 \cdot (1 - \exp(-[\tau_i/\beta]^\alpha))\} \\ &= -\lambda_0 \cdot w_n + \frac{\beta \cdot \lambda_0}{\alpha} \cdot \Gamma\left(\frac{1}{\alpha}\right) \cdot \sum_{i=1}^n G_{1/\alpha, 1}([\tau_i/\beta]^\alpha) + n \cdot \log \lambda_0 + \sum_{i=1}^n \log(1 - \exp(-[\tau_i/\beta]^\alpha)) \end{aligned}$$

where $G_{a, b}(\cdot)$ is the cumulative distribution function of $\text{gamma}(a, b)$. Then

$$\frac{\partial \log L(\lambda_0, \alpha, \beta | H_t)}{\partial \lambda_0} = -w_n + \frac{\beta}{\alpha} \cdot \Gamma\left(\frac{1}{\alpha}\right) \cdot \sum_{i=1}^n G_{1/\alpha, 1}([\tau_i/\beta]^\alpha) + n/\lambda_0 = 0$$

$$\begin{aligned} \frac{\partial \log L(\lambda_0, \beta | H_t)}{\partial \beta} &= \frac{\lambda_0}{\alpha} \cdot \Gamma\left(\frac{1}{\alpha}\right) \cdot \sum_{i=1}^n G_{1/\alpha, 1}([\tau_i/\beta]^\alpha) - \frac{\lambda_0}{\beta^\alpha} \cdot \sum_{i=1}^n \tau_i^\alpha G_{1/\alpha, 1}([\tau_i/\beta]^\alpha) \\ &\quad - \frac{\alpha}{\beta^{\alpha+1}} \sum_{i=1}^n \frac{\tau_i^\alpha \cdot \exp(-[\tau_i/\beta]^\alpha)}{1 - \exp(-[\tau_i/\beta]^\alpha)} = 0, \end{aligned}$$

where $G_{a, b}(\cdot)$ is the probability density function of $\text{gamma}(a, b)$. Hence $\hat{\lambda}_0$ can be expressed as a function of $\hat{\alpha}$ and $\hat{\beta}$ as follows:

$$\hat{\lambda}_0 = n / (w_n - \frac{\hat{\beta}}{\hat{\alpha}} \cdot \Gamma\left(\frac{1}{\hat{\alpha}}\right) \cdot \sum_{i=1}^n G_{1/\hat{\alpha}, 1}([\tau_i/\hat{\beta}]^{\hat{\alpha}})),$$

and the maximum log-likelihood (m.l.l.) is

$$\log L(\hat{\lambda}_0, \hat{\alpha}, \hat{\beta} | H_t) = -n + n \cdot \log \hat{\lambda}_0 + \sum_{i=1}^n \log(1 - \exp(-[\tau_i/\hat{\beta}]^{\hat{\alpha}})).$$

TABLE I

$\hat{t}_d=1.510$				$\hat{t}_d=1.630$			
$\hat{\alpha}$	$\hat{\beta}$	$\hat{\lambda}_0$	m.l.l.*	$\hat{\alpha}$	$\hat{\beta}$	$\hat{\lambda}_0$	m.l.l.*
0.500	20.000	0.2264	-6361.810	0.500	20.000	0.2295	-6344.262
1.000	20.000	0.3382	-6118.952	1.000	20.000	0.3438	-6108.733
1.500	10.500	0.2443	-6026.363	1.500	10.000	0.2384	-6019.673
2.000	8.500	0.2172	-5977.462	2.000	8.000	0.2095	-5973.962
2.500	7.500	0.2007	-5959.430	2.500	7.500	0.2045	-5958.362
3.000	7.000	0.1927	-5960.519	3.000	7.000	0.1963	-5961.747
3.500	6.500	0.1832	-5972.635	3.500	6.500	0.1866	-5974.956

$\hat{t}_d=1.750$				$\hat{t}_d=1.870$			
$\hat{\alpha}$	$\hat{\beta}$	$\hat{\lambda}_0$	m.l.l.*	$\hat{\alpha}$	$\hat{\beta}$	$\hat{\lambda}_0$	m.l.l.*
0.500	20.000	0.2327	-6326.689	0.500	20.000	0.2360	-6309.099
1.000	20.000	0.3495	-6098.800	1.000	20.000	0.3554	-6089.185
1.500	9.500	0.2324	-6013.277	1.500	9.500	0.2365	-6006.883
2.000	8.000	0.2133	-5970.306	2.000	8.000	0.2173	-5967.642
2.500	7.000	0.2960	-5958.133	2.500	7.000	0.1996	-5957.358
3.000	6.500	0.1875	-5963.839	3.000	6.500	0.1910	-5965.192
3.500	6.500	0.1901	-5979.156	3.500	6.500	0.1937	-5985.370

$\hat{t}_d=1.990$				$\hat{t}_d=2.110$			
$\hat{\alpha}$	$\hat{\beta}$	$\hat{\lambda}_0$	m.l.l.*	$\hat{\alpha}$	$\hat{\beta}$	$\hat{\lambda}_0$	m.l.l.*
0.500	20.000	0.2394	-6291.509	0.500	20.000	0.2429	-6273.940
1.000	19.000	0.3475	-6079.888	1.000	18.000	0.3394	-6070.737
1.500	9.000	0.2304	-6000.857	1.500	9.000	0.2345	-5995.220
2.000	7.500	0.2094	-5964.530	2.000	7.500	0.2132	-5962.579
2.500	7.000	0.2034	-5958.025	2.500	6.500	0.1948	-5958.601
3.000	6.500	0.1946	-5968.337	3.000	6.500	0.1983	-5973.441
3.500	6.500	0.1974	-5993.758	3.500	6.500	0.2012	-6004.514

$\hat{t}_d=2.230$				$\hat{t}_d=2.350$			
$\hat{\alpha}$	$\hat{\beta}$	$\hat{\lambda}_0$	m.l.l.*	$\hat{\alpha}$	$\hat{\beta}$	$\hat{\lambda}_0$	m.l.l.*
0.500	20.000	0.2464	-6256.418	0.500	20.000	0.2500	-6238.996
1.000	16.500	0.3237	-6061.763	1.000	15.500	0.3146	-6053.057
1.500	8.500	0.2281	-5089.773	1.500	8.000	0.2217	-5985.064
2.000	7.000	0.2053	-5960.681	2.000	7.000	0.2091	-5959.875
2.500	6.500	0.1984	-5960.027	2.500	6.500	0.2022	-5963.477
3.000	6.500	0.2021	-5980.729	3.000	6.500	0.2060	-5990.557
3.500	6.500	0.2051	-6017.904	3.500	6.500	0.2091	-6034.336

$\hat{t}_d=2.470$				$\hat{t}_d=2.590$			
$\hat{\alpha}$	$\hat{\beta}$	$\hat{\lambda}_0$	m.l.l.*	$\hat{\alpha}$	$\hat{\beta}$	$\hat{\lambda}_0$	m.l.l.*
0.500	20.000	0.2537	-6221.790	0.500	20.000	0.2576	-6205.728
1.000	14.500	0.3052	-6044.854	1.000	13.500	0.2954	-6039.025
1.500	8.000	0.2257	-5981.098	1.500	7.500	0.2190	-5980.863
2.000	6.500	0.2011	-5960.221	2.000	6.500	0.2049	-5965.377
2.500	6.500	0.2060	-5969.591	2.500	6.500	0.2100	-5983.107
3.000	6.500	0.2100	-6003.691	3.000	6.500	0.2141	-6025.826
3.500	6.500	0.2133	-6054.716	3.500	6.500	0.2175	-6085.680

*m.l.l is the abbreviation for *maximum log-likelihood* within the same ($\hat{t}_d, \hat{\alpha}, \hat{\beta}, \hat{\lambda}_0$) combination.

TABLE II

$\hat{t}_d=0.180$				$\hat{t}_d=0.260$			
$\hat{\alpha}$	$\hat{\beta}$	$\hat{\lambda}_0$	m.l.l.*	$\hat{\alpha}$	$\hat{\beta}$	$\hat{\lambda}_0$	m.l.l.*
2.000	7.000	1.0732	-3719.347	2.000	7.000	1.1124	-3697.096
2.500	7.000	1.3350	-3556.148	2.500	7.000	1.3919	-3538.967
3.000	7.000	1.6192	-3455.034	3.000	7.000	1.6961	-3443.885
3.500	7.000	1.9214	-3405.447	3.500	6.900	1.9414	-3401.172
4.000	6.200	1.5477	-3389.446	4.000	6.000	1.4840	-3387.642
4.500	5.600	1.2548	-3385.999	4.500	5.500	1.2558	-3386.692
5.000	5.000	1.1340	-3391.928	5.000	5.200	1.1322	-3394.249

$\hat{t}_d=0.340$				$\hat{t}_d=0.420$			
$\hat{\alpha}$	$\hat{\beta}$	$\hat{\lambda}_0$	m.l.l.*	$\hat{\alpha}$	$\hat{\beta}$	$\hat{\lambda}_0$	m.l.l.*
2.000	7.000	1.1547	-3675.162	2.000	7.000	1.1992	-3653.584
2.500	7.000	1.4521	-3522.409	2.500	7.000	1.5158	-3506.528
3.000	7.000	1.7778	-3433.679	3.000	7.000	1.8649	-3424.482
3.500	6.700	1.8826	-3397.509	3.500	6.500	1.8236	-3394.289
4.000	5.800	1.4214	-3386.317	4.000	5.600	1.3600	-3385.552
4.500	5.400	1.2567	-3387.280	4.500	5.200	1.1938	-3388.653
5.000	5.100	1.1302	-3397.263	5.000	4.900	1.0686	-3400.661

$\hat{t}_d=0.500$				$\hat{t}_d=0.580$			
$\hat{\alpha}$	$\hat{\beta}$	$\hat{\lambda}_0$	m.l.l.*	$\hat{\alpha}$	$\hat{\beta}$	$\hat{\lambda}_0$	m.l.l.*
2.000	7.000	1.2462	-3632.410	2.000	7.000	1.2958	-3611.699
2.500	7.000	1.5834	-3491.386	2.500	7.000	1.6551	-3477.063
3.000	7.000	1.9575	-3416.372	3.000	7.000	1.0562	-3409.448
3.500	6.200	1.6905	-3391.508	3.500	6.000	1.6324	-3389.273
4.000	5.500	1.3646	-3385.238	4.000	5.300	1.3035	-3385.638
4.500	5.100	1.1939	-3390.782	4.500	4.900	1.1328	-3393.625
5.000	4.800	1.0661	-3404.775	5.000	4.700	1.0634	-3409.801

$\hat{t}_d=0.660$				$\hat{t}_d=0.740$			
$\hat{\alpha}$	$\hat{\beta}$	$\hat{\lambda}_0$	m.l.l.*	$\hat{\alpha}$	$\hat{\beta}$	$\hat{\lambda}_0$	m.l.l.*
2.000	7.000	1.3482	-3591.532	2.000	7.000	1.4036	-3572.041
2.500	7.000	1.7311	-3463.665	2.500	7.000	1.8119	-3451.365
3.000	7.000	2.1614	-3403.841	3.000	7.000	2.2737	-3399.760
3.500	5.800	1.5744	-3387.701	3.500	5.600	1.5166	-3386.985
4.000	5.200	1.3070	-3386.838	4.000	5.000	1.2465	-3388.953
4.500	4.800	1.1321	-3397.238	4.500	4.700	1.1312	-3402.142
5.000	4.500	1.0044	-3415.683	5.000	4.400	1.0014	-3422.570

$\hat{t}_d=0.820$				$\hat{t}_d=0.900$			
$\hat{\alpha}$	$\hat{\beta}$	$\hat{\lambda}_0$	m.l.l.*	$\hat{\alpha}$	$\hat{\beta}$	$\hat{\lambda}_0$	m.l.l.*
2.000	7.000	1.4621	-3553.528	2.000	7.000	1.5241	-3537.807
2.500	7.000	1.8978	-3440.542	2.500	7.000	1.9891	-3433.472
3.000	6.700	2.1463	-3397.225	3.000	6.300	1.9451	-3398.467
3.500	5.400	1.4990	-3387.614	3.500	5.200	1.4019	-3392.728
4.000	4.900	1.2489	-3392.758	4.000	4.700	1.1892	-3401.503
4.500	4.500	1.0716	-3408.536	4.500	4.400	1.0701	-3420.753
5.000	4.300	0.9982	-3431.461	5.000	4.200	0.9950	-3446.830

*m.l.l is the abbreviation for *maximum log-likelihood* within the same $(\hat{t}_d, \hat{\alpha}, \hat{\beta}, \hat{\lambda}_0)$ combination.

Figure Legend

Fig. 1

This is the procedure outline flow-chart.

Fig. 2

In each column, (a) is the correlogram, (b) is the conditional mean plot with fixed cellsize. The correlogram is done by plotting the sample correlation coefficients up to order 20 against their orders. The conditional mean plots in (b) are constructed by first grouping the pairs (τ_n, τ_{n+1}) with respect to the magnitude of the first component τ_n such that approximately equal number of pairs are in each group. Then plot the means of the second components τ_{n+1} against the midpoints of the intervals in which their partners τ_n fell in. In (b), the cellsize for NERVE1 and NERVE2 are 40 and 50, respectively.

Fig. 3

These are the conditional interval histograms for: (a), the original NERVE1, and (b), the simulated NERVE1. There are 400 interspike intervals in each histograms and the mean conditioning interval lengths are arranged in an increasing order.

Fig. 4

The conditional interval histograms for: (a) original NERVE2; (b) whitened NERVE2; and (c) simulated NERVE2. There are 400 observations in each histogram.

Fig. 5

This is the conditional mean plot for the pairs $(\tau_n, \log(\tau_{n+1}))$ rather than for the original pairs.

Fig. 6

The hazard rate plot with the hypothesized intensity function of NERVE1. The binwidth is 1.0.

Procedures outline flow chart

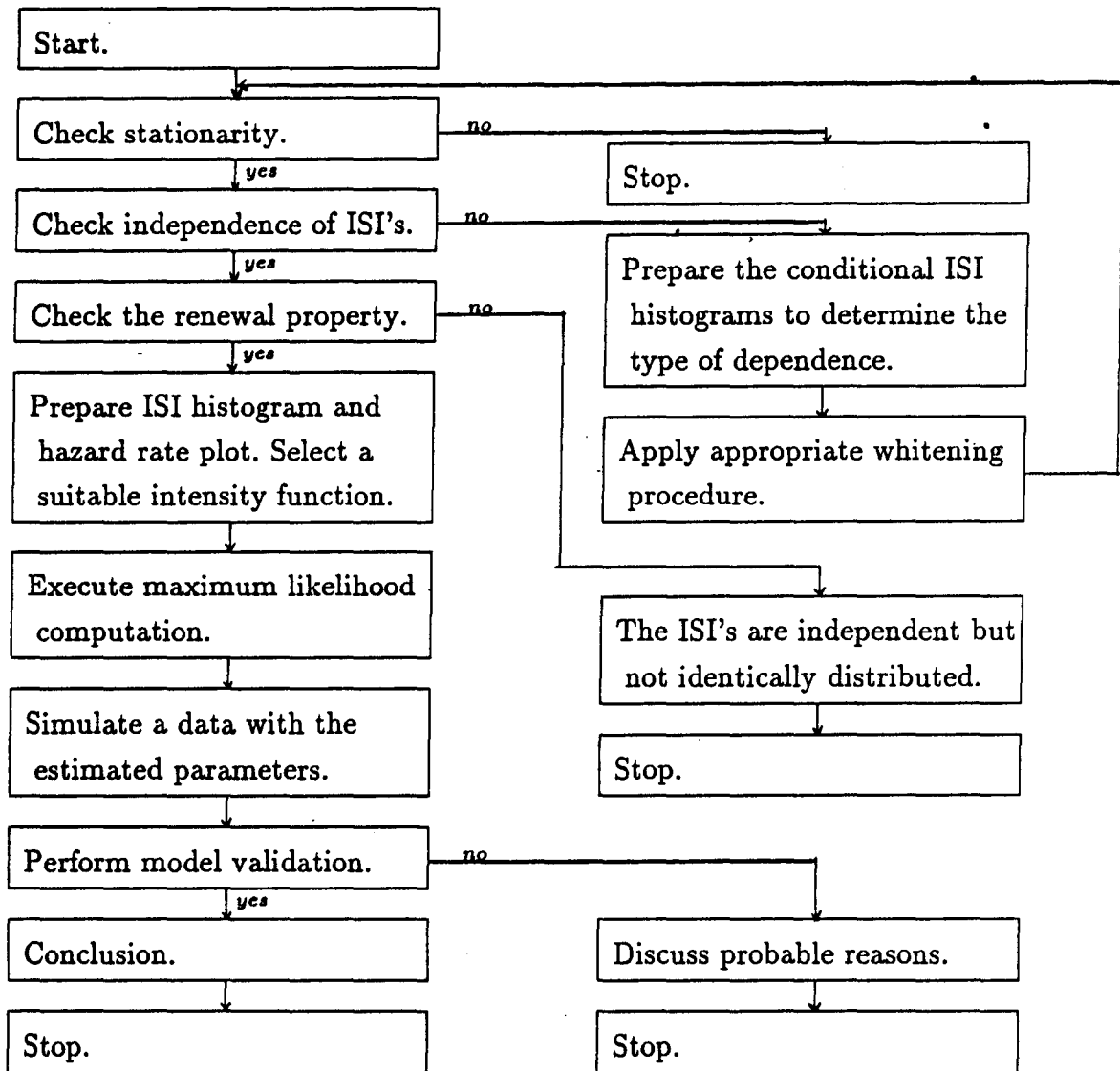


Fig. 1

CORRELOGRAM OF NERVE1

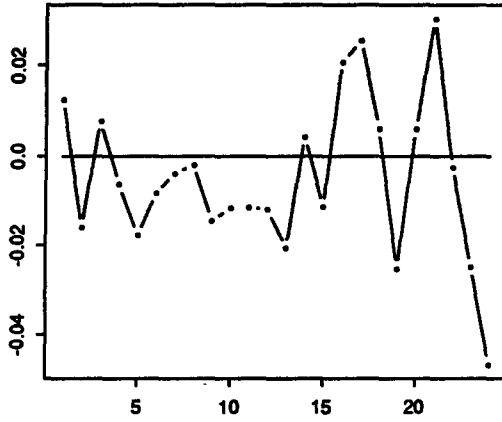


Fig. 2.1(a)

COND. MEAN PLOT OF NERVE1

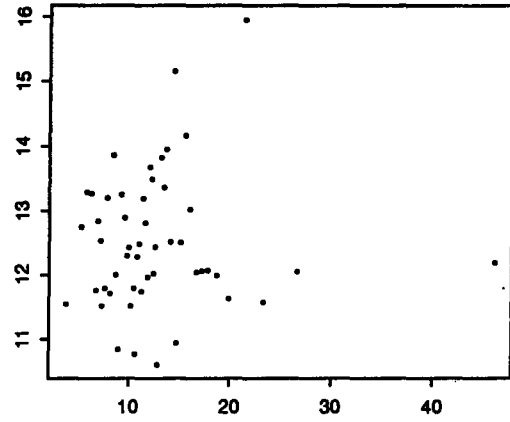


Fig. 2.1(b)

CORRELOGRAM OF NERVE2

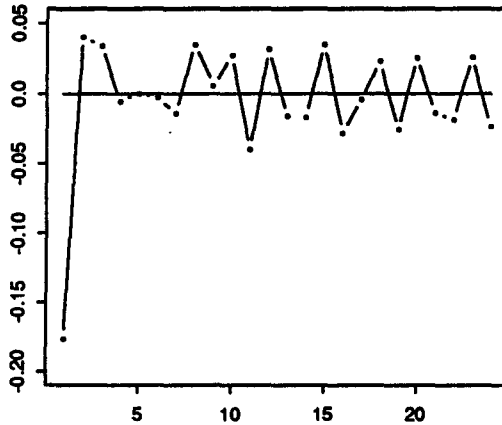


Fig. 2.2(a)

COND. MEAN PLOT OF NERVE2

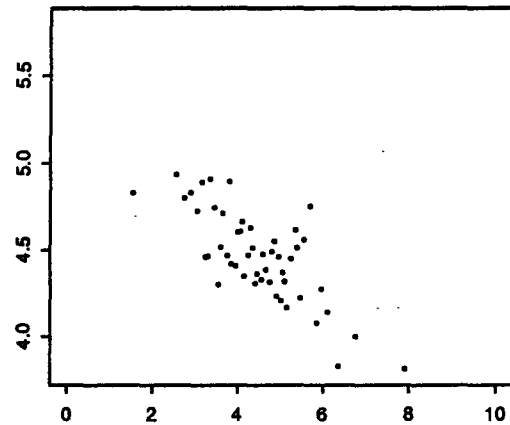


Fig. 2.2(b)

CORRELOGRAM OF WHITENED NERVE2

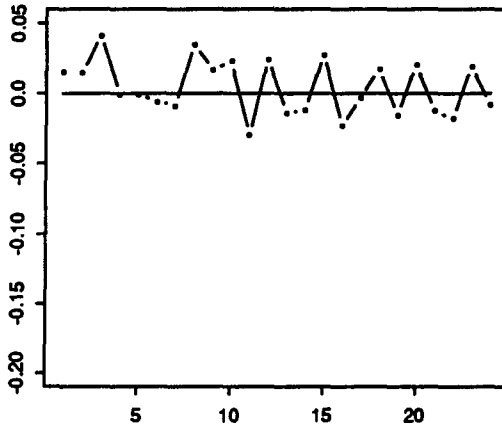


Fig. 2.3(a)

COND. MEAN PLOT OF WHITENED NERVE2

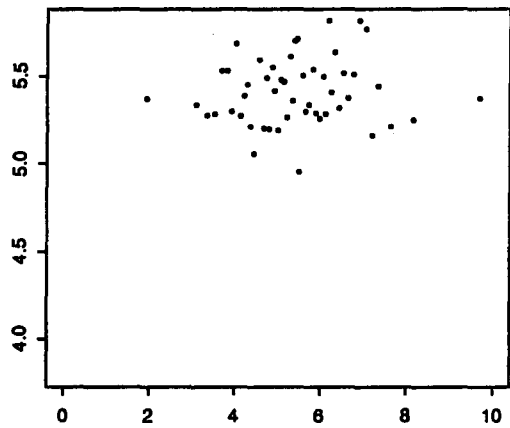
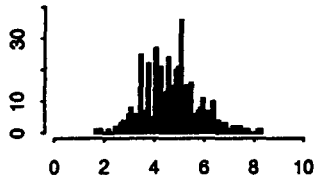


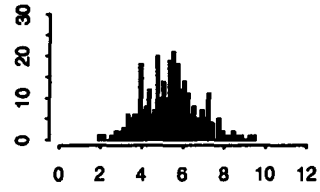
Fig. 2.3(b)

Fig. 2

ORIGINAL NERVE2



WHITENED NERVE2



SIMULATED NERVE2

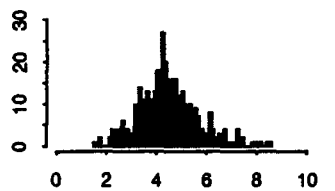
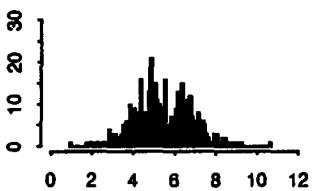
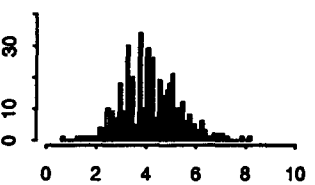
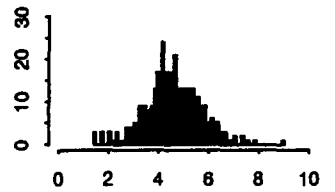
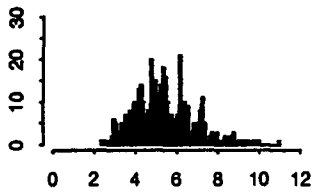
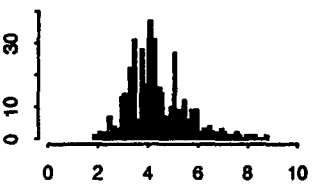
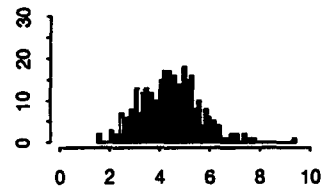
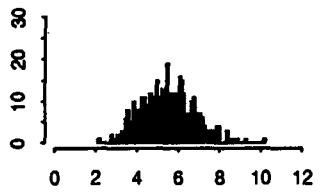
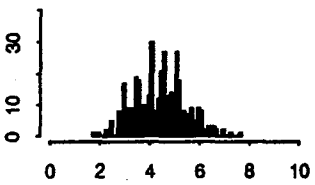
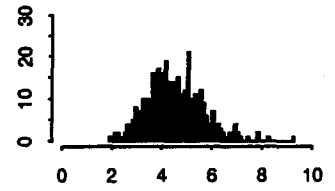
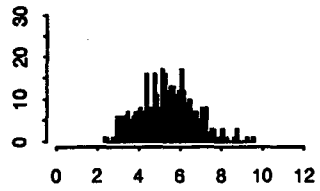
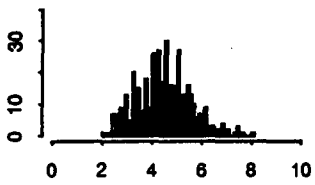
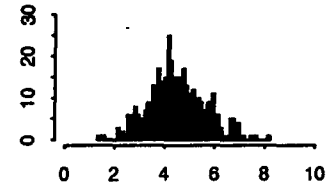


Fig. 4(a)

Fig. 4(b)

Fig. 4(c)

Fig. 4

SEMI-LOG CONDITIONAL MEAN PLOT OF NERVE2

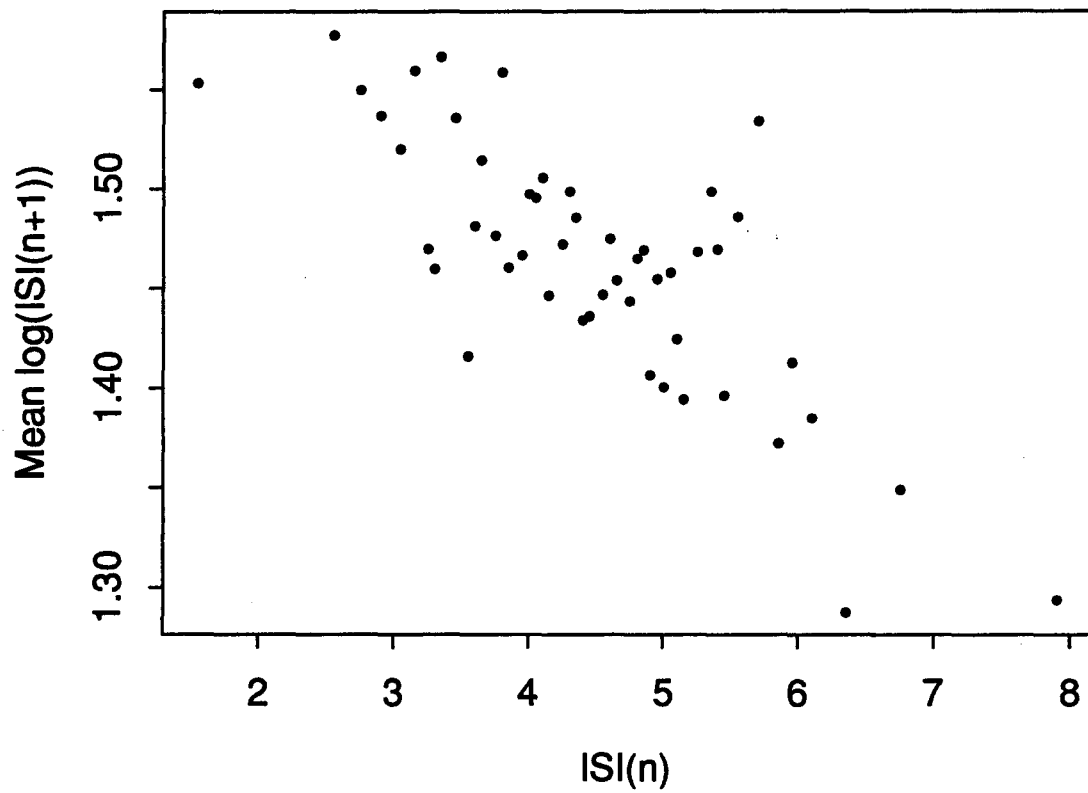


Fig. 5

HAZARD RATE PLOT OF NERVE1

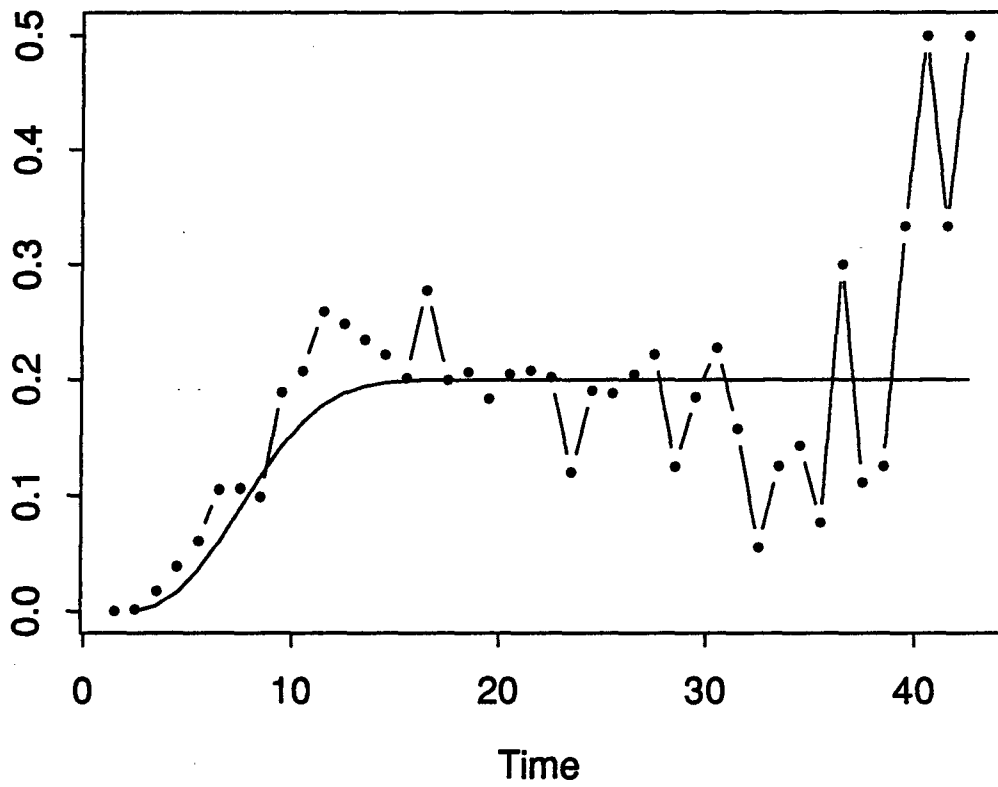


Fig. 6

References

- Bi, Q., 1989, 'A Closed-form Solution for Removing the Dead-time Effects from the Poststimulus Time Histograms' J. Acoust. Soc. Am. 85(6), 2504-2513
- Correia, B. J., and Landolt, J. P., 1977, 'A Point Process Analysis of the Spontaneous Activity of Anterior Semicircular Canal Units in the Anesthetized Pigeon' Biol. Cybern. 27, 199-213
- Cox, D. R., and Isham, V., 1980, 'Point Processes' Chapman and Hall
- Cox, D. R., and Lewis, P. A. W., 1966, 'The Statistical Analysis of Series of Events' Methuen, London
- Fuller, W. A., 1976, 'An Introduction to Statistical Time Series Analysis' Wiley, New York
- Johnson, D. H., and Swami, A., 1983, 'The Transmission of Signals by Auditory-Nerve Fiber Discharge Patterns' J. Acoust. Soc. 74(2), 493-501
- Johnson, D. H., Tsuchitani, C., Linebarger, D. A., and Johnson, M. J., 1986 'Application of a Point Process Model to Responses of Cat Lateral Superior Olive Units to Ipsilateral Tones' Hearing Research 21, 135-159
- Kiang, N. Y. S., Watanabe, T., Thomas, E. C., and Clark, L. F., 1965, 'Discharge Patterns of Single Fibers in the Cat's Auditory Nerve' M.I.T., Cambridge, MA
- Kwaadsteniet, J. W. de, 1982, 'Statistical Analysis and Stochastic Modeling of Neuronal Spike-train Activity' Math. Biosc. 60, 17-71
- Landolt, J. P., and Correia, M. J., 1978, 'Neuromathematical Concepts of Point Process Theory' IEEE Trans. Biomed. Eng. BME-25,1-12
- Ogata, Y., 1978, 'Asymptotic Behavior of Maximum Likelihood Estimators for Stationary Point Processes' Ann. Inst. Stat. Math. 30, A, 243-261
- Ozaki, T., 1979, 'Maximum Likelihood Estimation of Hawkes' Self-exciting Point Processes' Ann. Inst. Stat. Math. 31, B, 145-155
- Perkel, D. H., Gerstein, G. L., and Moore, G. P., 1967, 'Neural Spike Trains and Stochastic Point Processes' Biophysical J. 7, 4, 391-418

- Smith, C. E., and Chen, C. L., 1986, '*Serial Dependency in Neural Point Processes due to Cumulative Afterhyperpolarization*' Institute of Statistics Mimeo Series No. 1691, North Carolina State University, Raleigh, North Carolina
- Smith, C. E., and Goldberg, J. M., 1986, '*A Stochastic Afterhyperpolarization Model for Repetitive Activity in Vestibular Afferents*' Biol. Cybern. 54, 41-51
- Snyder, D. L., 1975, '*Random Point Processes*' Wiley and Sons, New York
- Tuckwell, H. C., 1988, '*Introduction to Theoretical Neurobiology, Vol. 2*' Cambridge University Press, Cambridge
- Yang, G. L., and Chen, T. C., 1978, '*On Statistical Methods in Neuronal Spike-train Analysis*' Math. Biosc. 38, 1-34
- Yang, X., and Shamma, S. A., 1990, '*Identification of Connectivity in Neural Networks*' Biophys J. Vol. 57, 987-999